

Evaluating Miniature Robot Surgical Scissors*

Zhuo Fan Bao¹ and Eric Diller¹

Abstract—Proper methods are not available to evaluate miniature robot surgical scissors' abilities. This paper proposes agar gel as a reference cutting material for comparison between miniature robot surgical scissors of different designs. Trends in material properties (yield strength and fracture toughness) of agar were determined to correlate positively with its concentration by weight through experimentation. This indicates that agar tends to become more resistant to fracture nucleation and crack propagation with increasing agar concentration. Then, using novel magnetic robot surgical scissors, a cutting test showcased a positive correlation between agar cutting difficulty and its concentration. Thus, given increasing difficulty to cut with increasing agar concentration, agar gel could serve as a potential standard to compare miniature robot surgical scissors cutting capabilities.

I. INTRODUCTION

As minimally invasive surgery becomes more common, surgeons require a multitude of tools adapted to minimally invasive surgery to facilitate the surgical process. Magnetically actuated untethered tools have emerged as a potential solution to minimally invasive surgery due to their low mechanical footprint and remote actuation power delivery through magnetic fields. In recent years, there has been significant development in the magnetic microrobotics field that can enable operations at the small scale, including biopsy [1], suturing [2], [3], cutting [4] and grasping [5]. However, surface friction becomes a significant obstacle to actuation as power sources tend to scale down at a faster rate than friction. Friction is especially challenging for miniature scissors: proper blade contact is necessary to generate enough shearing force to nucleate fracture, but it would introduce friction that could overwhelm limited actuation force. Coupled with a complex soft tissue cutting mechanism that is poorly understood [6] even at the macro scale, surface friction poses serious challenges to developing reliable and strong miniature scissors for soft tissue cutting.

Despite these challenges, a previous study demonstrated a proof-of-concept magnetically actuated centimeter-scale untethered scissors that could cut agar [4]. The proposed scissors leveraged the combination of on board magnets and a nickel titanium (nitinol) spring to open and close its jaws. Furthermore, it was capable of untethered locomotion in the workspace through a crawling motion. However, the untethered nature of such a tool limited its controllability, and the scissors only had 35 mN of available cutting force.

*We acknowledge the support of the Natural Sciences and Engineering Research Council of Canada (NSERC)

¹Zhuo Fan Bao and Eric Diller are with the Department of Mechanical and Industrial Engineering, University of Toronto, 5 King's College Rd, Toronto, ON M5S 3G8, Canada zbao@mie.utoronto.ca, ediller@mie.utoronto.ca

The current study aims to complement this development in miniature robot surgical scissors through establishing a reference material for evaluating scissors cutting at the small scale. Agar gel will be considered in the scope of this study because agarose gel, a purified form of agar, is often used as an analog for brain tissues [7], but agar is more accessible and is already primarily made up of agarose. Agar gel property characterization works are sparse and dated in literature [8]. Thus, this work will evaluate the macro material properties (yield strength & fracture toughness) of agar to verify if at the small scale, they are good indicators of scissors cutting difficulty. This work is motivated by the lack of a proper standard to evaluate miniature robotic scissors cutting in the literature. Works detailing scissors cutting tend to report on the forces necessary to cut as they were developed for haptics feedback [9], [10], [11] rather than for tool performance characterization and comparison. A variety of factors beyond force can affect untethered soft tissue cutting. The blade's sharpness [12], the blade's movement [13], [14] and the scissors' geometry [15] could affect the cutting mechanics. As such, scissors should be evaluated based on the resistance to scissors cutting of reference materials they are trying to cut instead of the scissors' force output. This would enable comparison between miniature robot surgical scissors that leverage a variety of actuation methods and designs.

Previous work has attempted to rank the fracture toughness of thin mammalian soft tissues based on scissors cutting [16]. This work will attempt to develop an evaluation approach for miniature robot surgical scissors based on using agar as a reference material for ranking scissors cutting difficulty. To do so, the yield strength and fracture toughness of agar samples of various concentrations are determined experimentally through tensile and J-integral testing. Tensile testing evaluates the stress response of a material to tension. Yield strength is the maximum recorded stress before breakage of a material in tensile testing and is an indicator of the material's resistance to fracture nucleation. J-integral is a representation of the strain energy necessary for crack propagation [17].

After determining their material properties, the agar samples are ranked in difficulty based on the field strength needed to cut them in a cutting test featuring novel miniature robot surgical scissors with reduced size and improved blades. Based on the results of the test, this study will attempt to draw correlations between the agar concentration and the difficulty of cutting to develop a standard against which miniature robot surgical scissors of different designs and actuation could be evaluated against.

II. AGAR CHARACTERIZATION

The process of determining the yield strength and fracture toughness of agar gel in this work is derived from previous works [18], [19]. The characterization procedure was developed for agarose gel, but due to its similar nature to agar, this work will extend its application to agar gel as well. Tensile testing first establishes the stress-strain relationships of agar and determines its yield strength. Subsequently, digital image correlation (DIC) was used to determine the critical J-integral of agar gel. DIC is a vision-based displacement measurement technique that compares between video frames to determine the displacement of the material based on pattern recognition algorithms. Vision-based techniques are preferred for characterizing soft materials as material contact is difficult to determine using conventional measurement techniques [19].

A. Tensile Testing

Tensile testing is conducted to determine the yield strength and the stress-strain relationship of agar gel. The stress-strain relationship is necessary for computing the J-integral values of agar in the subsequent J-integral testing. A previous study [18] determined that agarose stress-strain curves behave according to a second order equation, which was used to fit the experimental data:

$$\sigma = c_1\epsilon + c_2\epsilon^2, \quad (1)$$

where c_1 and c_2 are constants obtained from fitting the stress-strain curve, σ is stress in Pa and ϵ is strain.

B. J-integral Test

J-integral was developed in the 1960s as a method to evaluate energy release of a crack or notch because the high levels of strain that occur near the crack tip makes them difficult to determine directly [17]. J-integral is a contour path integral surrounding the crack in a 2D plane. It is path independent, and would allow the evaluation of the strain energy required to propagate said crack without having to measure crack tip strain. Fracture toughness can be inferred from the critical J-integral, which is a discontinuity in a J-integral plot over time due to yielding in a brittle material.

J-integral was combined with modern vision-based pattern recognition techniques to develop a method to evaluate the fracture toughness of hydrogel using a camera. An attempt to evaluate the fracture toughness of agar will be based on the methods and equations presented in [19].

III. EXPERIMENTAL SETUP

The experimental procedure of this study involved first preparing agar samples, which were used to determine their yield strength and fracture toughness. After characterization, agar samples were then subject to a cutting test featuring novel miniature robot surgical scissors to determine difficulty of cutting.

A. Agar Preparation

Agar (Sigma-Aldrich) and water mixtures were boiled, cooled and weighed before being poured into 3D printed resin molds (Clear V4, Formlabs) and refrigerated. The agar was dyed using a drop of food coloring for better contrast. To ensure minimal dehydration during refrigeration, agar samples were tested within 2 – 3 hours after casting.

3D printed molds were designed to shape the agar depending on the experiment. For tensile testing, specimens were molded with two shoulders and a gage (Fig. 1 (a)) to promote breakage in the gage section. For the J-integral testing, agar was molded into blocks (Fig. 1 (b)) so they can be notched right before testing. The cutting experiment used 1.7 mm thin slices of agar of various length cut from a pre-molded strip. A slight 1° draft angle was added to all molds to aid removal from the mold.

B. Agar Characterization

Both agar characterization experiments (tensile & J-integral test) were conducted on a single linear rail of a three-axis gantry system (FuyuMotion) with motor drivers controlled by an Arduino (Arduino Mega).

1) *Tensile Testing*: Special clamps to hold the agar were 3D printed and faced with sand paper on the inside to improve grip (Fig. 1 (c)). Force measurements were recorded using a load cell (single axis 500 g GSO Load Cell + Burster DAQ) and were synchronized against positional data of the gantry through custom built software. The force sensor was calibrated before every set of experiment. The crosshead speed for this experiment was set to 0.2 mm/s or 100 steps/s and ran until breakage of the specimen. Resolution of the gantry limited the speed to no slower than 0.2 mm/s. Previous work observed stress-strain values to be insensitive to crosshead speeds once below 1.7 mm/s [19].

Force measurements were divided by the cross-section area of the gage to compute stress as:

$$\sigma = \frac{F_{\text{loadcell}}}{3 \text{ mm} \times 10 \text{ mm}}. \quad (2)$$

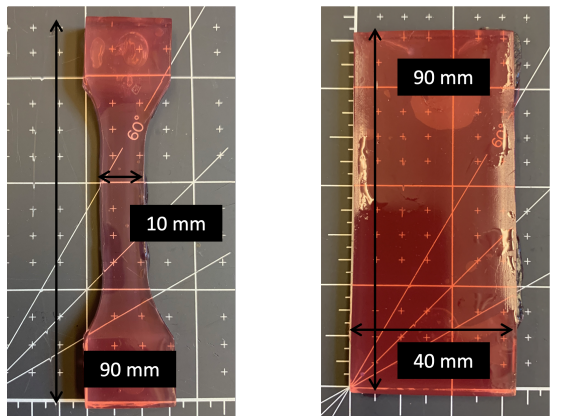
Strain values were computed from the digital encoded step values reported by the Arduino:

$$\epsilon = \frac{(L - L_0)}{30 \text{ mm}}. \quad (3)$$

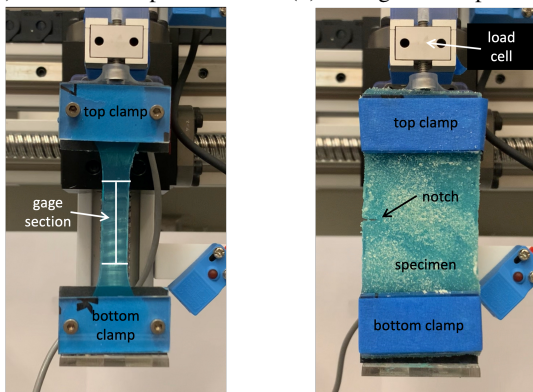
The stress-strain curve was fitted to Eq. 1. The range of the fitting is selected manually to avoid going beyond the elastic region of the deformation as shown in Fig. 4.

2) *J-Integral Test*: To pattern the specimen for DIC, the specimen was coated with agar powder (Fig. 1 (d)). After it was loaded, a sharp razor blade was used to notch the specimen. The specimens were then pulled at a rate of 0.2 mm/s until complete fracture while footage was recorded using a camera running at 30 frames per second (fps).

Post-processing of the recorded footage began with trimming unnecessary footage. Frames were extracted every 0.1 s, and pictures were cropped leaving the notch in focus. The frames were fed through an open source package



(a) Tensile test specimen. (b) J-integral test specimen.



(c) Tensile test setup. (d) J-integral test setup.

Fig. 1. Test setup for measuring agar material properties: (a) Tensile testing specimen used to measure the yield strength of agar. It has shoulders to promote breakage in the gage section, which is 10 mm wide and 3 mm thick. (b) The J-integral testing specimen is a block of 5 mm thick agar. The agar is notched only after it is loaded onto the experimental setup. (c) Tensile testing agar specimen clamped between 3D printed clamps lined with sand paper and held together using M3 screws. The silver rectangle at the top of the figure is the GSO load cell. The direction of pull is towards the top of the picture. (d) Agar specimen clamped for J-integral test and patterned using agar powder for DIC. The specimen is notched on the left side using a razor blade immediately before the beginning of the test.

(NCorr [20]) for DIC, and the displacement and strain values were used by a self-implemented script of the equations from [19] to determine the critical J-integral.

C. State-of-the-art scissors

The scissors (Fig. 2) for the cutting experiment are designed based on the untethered surgical scissors [4] with some notable design improvements, including a 30% reduction in width, and upgraded blades. The width of the scissors are 7 mm across its widest side, and the blades have been updated with off-the-shelf titanium scalpel blades to reduce unwanted magnetic interactions during actuation. The construction of the scissors consists of a 3D printed (Clear V4, FormLabs) pin joint body with slots for blades and magnets. Both jaws of the scissors have a wedge shaped profile to prevent the jaws from getting caught during cutting. The scissors' body is printed in halves for an improved print quality and simplified blade assembly. Along with the blades, the scissors body is glued together using cyanoacrylate glue

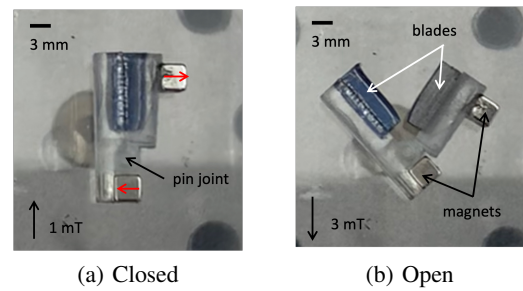


Fig. 2. Fully assembled novel robot scissors (direction and magnitude of field currently applied in bottom left corner): (a) Scissors closed from an uniform field of 1 mT pointing away from the jaws. The red arrows indicate the direction of magnetization of the magnets. (b) Scissors' jaw opening from an uniform field of 3 mT pointing into the jaws.

(Gorilla Glue).

The blades (MRimed Disposable Titanium Scalpel Blade #15) are ground down to 0.01 m in length and sanded down on one side to reduce the bevel of the blade and improve blade edge contact. The specific blade model was chosen because it is nonmagnetic and because its asymmetric blade bevel reduces the amount of work necessary to convert them into scissor blades as grinding titanium can be quite challenging due to its hardness.

For actuation, a 3.18 mm cube neodymium iron boron (NdFeB) magnet (N42 grade, K&J Magnetics) is attached on each jaw of the scissors using epoxy glue (Gorilla Glue), resulting in a net zero magnetization when closed (Fig. 2 (a)). Scissors face difficulty when attempting to finish a cut as that is when the moment arm between the pivot point and cut location is longest. Therefore, the magnets are oriented to achieve maximum closing torque when closed to attempt to address this issue. A uniform field pointing from the pivot point towards the jaws closes them. Reversing the field opens the jaws (Fig. 2 (b)). Initial tests show that the scissors' jaws are capable of opening using a 3 mT field and closing using just 1 mT. Closing actuation requires a weaker field input because the magnets repel each other in the open configuration, creating a weak spring force that aids closing and assists with cutting.

The scissors in the current setup are unstable when closing. Due to manufacturing defects, the magnets are not perfectly in plane with the generated field, so the scissors tend to flip out of plane and also about the pivot axis, to assume an open jaws configuration in the opposite direction. Future work will aim to address this stability issue, but in the current study, cutting is conducted using tethered scissors where the base of the untethered scissors is taped to the end of a stirring rod. The implication of this adjustment are that gradients cannot be utilized to pull the scissors forward during the cut to prevent the material from slipping away from the jaws. Overall, the trends observed in this study should not be affected by this change in setup.

The actuation sequence for cutting using such scissors is broken down into three stages: open approach, catching and cutting. The scissors open and position themselves with the target cut material in between their jaws during the open

approach stage. The catching stage is when the scissors bite down onto the target to secure itself before increasing in cutting force. For materials with lower yield strength, the catching phase might nucleate fracture onto the target material due to the slight instantaneous force generated from the scissors clamping down. The bulk of cutting happens during the cutting stage where the scissors linearly increase in cutting force to finish the cut. The scissors are expected to encounter the most resistance at the beginning of the closing stage as the magnets are positioned to exert maximum torque when fully closed.

D. Cutting Setup

For the cutting experiment, the fields used to actuate the scissors were generated by an electromagnet system with eight coils [21]. The scissors sat on top of this system on an acrylic plate with a cut out size adjustable slot for clamping down 1.7 mm thin agar gel strips to cut (Fig. 3). To initiate cutting, the magnetic field, pointing in the direction from the pivot point of the scissors to their jaws, was increased linearly according to the following equation:

$$B = 0.5t - 3 \text{ mT}, \quad (4)$$

where B is the field magnitude in mT in the direction pointing away from the jaws of the scissors and t is time in s. The field would saturate at 20 mT and hold until cutting was complete, if necessary. The scissors actuated according to the sequence described in the above section based on this linearly increasing field. Between -3 mT and 0 mT, the scissors would be on the open approach. Catching would happen somewhere between 0 mT – 5 mT. Catching requires a stronger field than the reported closing field because depending on setup conditions, the scissors might need to overcome additional friction. Then, from 5 mT up to 20 mT, the scissors apply increasing cutting torque.

A gradually increasing field is preferred over a step increase in field strength as that would generate more impact force. While impact-based actuation could be leveraged to generate more instantaneous force in a cut [2], [22], the catching stage becomes uncontrollable. In the context of untethered scissors cutting, uncontrolled moving blades could be dangerous for adjacent tissues or to the section being cut by causing unnecessary damage, which could lead to complications. As such, impact based scissor actuation was not considered for testing in this study.

Footage of the scissors actuating under the increasing field was recorded at 30 fps, and the maximum field at which cutting is completed was determined qualitatively by inspection of video footage, and timestamps were used to determine the final applied field value.

IV. RESULTS

A. Tensile Testing

The stress-strain curves of tested agar gels were fitted (Fig. 4) and the maximum yield strength were extracted. A total of 21 tensile tests were recorded and were binned according to their agar weight % concentration. The mean yield

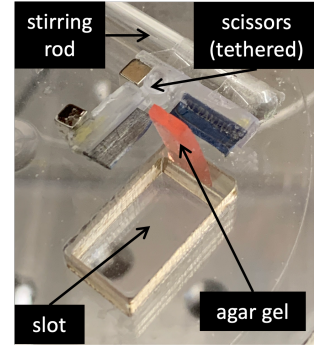


Fig. 3. Cutting setup: the agar dyed in red is held in place by a slot in the acrylic plate. The agar gel is lined up against the static jaw taped to the stirring rod. The scissors are taped down in the open configuration with the agar gel positioned as close to the pin joint of the scissors as possible.

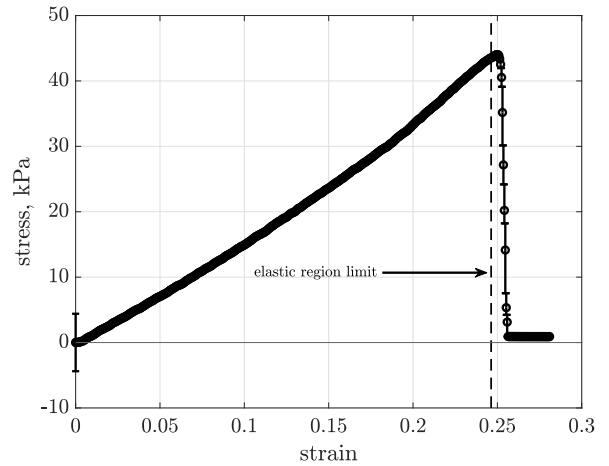


Fig. 4. Stress-strain curve: Sample strain-stress curve of 3.2% agar gel. The lack of a plastic deformation region demonstrates that the material is brittle. The elastic region limit indicates the curve fitting goes from 0 up to 0.246 in this plot.

strength of each bin was plotted against their concentration in Fig. 5 along with their respective standard deviation. The stress-strain curves (Fig. 4) confirm the brittleness of agar because no plastic deformation is observed.

The experimental yield strength of agar seems to agree with theory as it follows an increasing trend in the 1 – 3 % concentration region. The root mean square difference (RMSD) between the fit and the data points is 3.7 kPa.

High concentration agar is expected to be more resistant to fracture nucleation because yield strength appears to increase with agar concentration. This phenomenon was observed qualitatively during cutting testing where high concentration agar was noticeably more resilient to accidental damage during setup. However, further studies would be needed to confirm this.

B. J-integral test

The critical J-integral values (Fig. 6) were determined manually from J-integral plots of each test. A total of 15 J-integral tests were conducted and the data points were fit

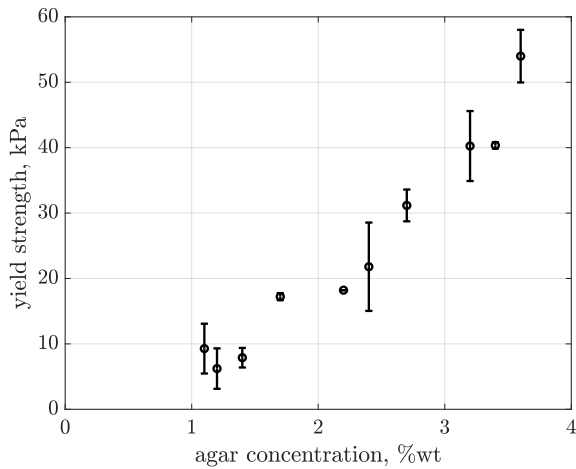


Fig. 5. Yield strength variation with respect to agar concentration: Data points plotted along with their respective standard deviation for agar samples of 1 – 3% concentration. The yield strength of agar seems to increase with increasing agar concentration.

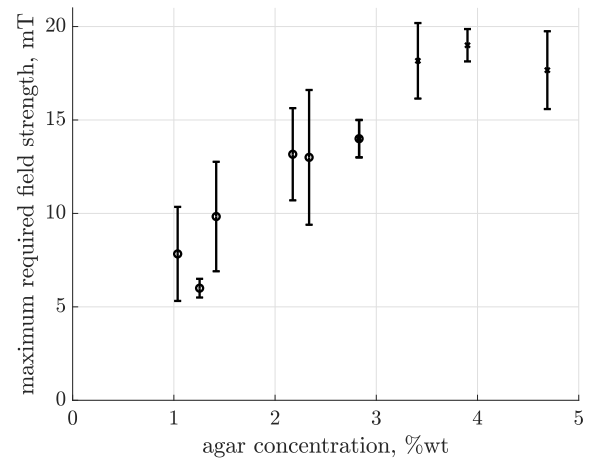


Fig. 7. Cutting difficulty with respect to agar concentration: The difficulty of cutting agar gels was determined based on the highest field magnitude required to complete the cut. Saturation occurs for data points where concentration > 3% (marked by an x) due to lack of a stronger field than 20 mT.

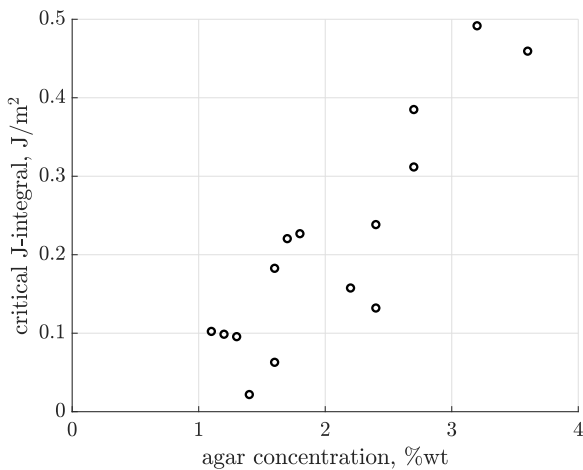


Fig. 6. Critical J-integral with respect to agar concentration: Critical J-integral values were extracted manually and plotted against their respective concentration. The scatter plot demonstrates an increasing trend with increasing concentration.

to a linear function, which had a RMSD of 65 mJ/m².

The critical J-integral is an indicator of the energy necessary to propagate a crack. Thus, the J-integral test results seem to indicate that more cutting force is required to cut through higher concentration agar. This was also observed qualitatively during the cutting test where despite initial fracture, the scissors required substantially more time to finish the cut, or in other words, a stronger field.

C. Cutting Test

The final maximum cutting force to complete a cut was computed and plotted against agar gel concentrations (Fig. 7). The plot shows an increasing trend of requiring stronger field input to cut at higher agar concentrations. This can be explained by the fact that a combination of higher

yield strength and fracture toughness at higher agar concentrations, demonstrated from the previous results, makes the agar substantially more resistant to fracturing and fracture propagation, and thus more difficult to cut.

Unfortunately, due to hardware limitations, the plot saturates at 20 mT for higher concentrations. The cuts are still considered complete as the field was left on at 20 mT until completion, but some cuts required upwards of an additional 20 s of field exposure to complete and thus are not representative of this linear trend. Nevertheless, these data points are still plotted (with an x) to showcase an overall increasing trend, but a more accurate linear fitting only considering 3% and lower agar concentrations is a better display of the trend. The RMSD of a $\leq 3\%$ concentration fit is lower than that of an overall fit (1.15 mT versus 1.61 mT).

These results confirm that agar concentration is positively correlated with miniature scissors cutting difficulty and that macro material properties such as yield strength and fracture toughness are valid fracture mechanics metrics at the small scale. The increasing cutting difficulty of agar at higher concentration can be leveraged to establish a benchmark for comparing cutting abilities of miniature scissors without relying on reporting force outputs. The amplitude of the required fields to cut help anticipate actuating field requirements for future magnetic actuated scissors development. While favourable, these results only serve to illustrate trends that relate fracture mechanics to the difficulty of executing a scissors cut at the small scale. Further work should be done to confirm these trends and numbers.

D. Limitations and future work

For the tensile testing in particular, while [18] describes a more complex tensile testing with DIC required to account for water leakage and volume decrease during testing that could cause uneven strain fields to form, this study only

computed stress-strain relationships based on observed overall displacement of the material, due to a lack of sufficiently accurate equipment to replicate the work done in [18] and because this study only seeks to establish trends in agar gel cutting to propose a potential method of evaluating scissors cutting. As such, some variation in the data can be observed. Further work with increased attention to accuracy should be conducted to further evaluate the material properties of agar. Based on the available literature [23], the current setup should still be sufficient to observe trends in agar yield strength with respect to its concentration.

The complexity of the setup and of the data post-processing for the J-integral testing made consistency a challenge. Due to the nature of image based techniques, some data points could not be resolved due to poor footage or setup and had to be discarded. As such, similar to the results from the tensile testing, the results from the J-integral testing are only relevant relative to each other rather than in an absolute context. Further work is required to properly understand the crack propagation mechanism of agar.

For the cutting experiment, the capability to apply input fields beyond 20 mT would confirm whether cutting difficulty remains linear past 3% agar concentration. Furthermore, during the cutting experiment, it was observed that several factors not considered in this study also played an important role in affecting a scissors cut, especially at the small scale. A notable qualitative observation is that the manner in which the scissors' blades are positioned with respect to the target cut material greatly affected the difficulty of the cut. As the setup for the cutting experiment became more rehearsed, the results obtained were noticeably more consistent (much lower RMSD if fitting to newer data points). A few data points were discarded during post-processing because they were suspected to be outliers due to faulty setup at the beginning of testing. Nevertheless, despite attempts to improve the setup, variations in the final cutting results were expected because even micro positional adjustments and movements during testing, such as the blade's angle of attack and distance of scissors from the target, could affect cutting. Further investigation would be necessary to better understand how the dynamics, speed and acceleration, and positioning of such scissors could be optimized to improve cutting.

ACKNOWLEDGMENT

The authors would like to thank Cameron Forbrigger, Chloe Pogue, Robin Liu and Monisha Naik for providing valuable insight and feedback.

REFERENCES

- [1] D. Ye, J. Xue, S. Yuan, F. Zhang, S. Song, J. Wang, and M. Meng, "Design and control of a magnetically-actuated capsule robot with biopsy function," *IEEE Transactions on Biomedical Engineering*, pp. 1–1, 2022.
- [2] O. Erin, X. Liu, J. Ge, J. Opfermann, Y. Barnoy, L. O. Mair, J. U. Kang, W. Gensheimer, I. N. Weinberg, Y. Diaz-Mercado, and A. Krieger, "Overcoming the force limitations of magnetic robotic surgery: Magnetic pulse actuated collisions for tissue-penetrating-needle for tetherless interventions," *Advanced Intelligent Systems*, vol. n/a, no. n/a, p. 2200072, 2022. [Online]. Available: <https://onlinelibrary.wiley.com/doi/abs/10.1002/aisy.202200072>
- [3] L. O. Mair, S. Chowdhury, X. Liu, O. Erin, O. Udalov, S. Raval, B. Johnson, S. Jafari, D. J. Cappelleri, Y. Diaz-Mercado, A. Krieger, and I. N. Weinberg, "Going hands-free: Magnetosuture for untethered guided needle penetration of human tissue ex vivo," *Robotics*, vol. 10, no. 4, 2021. [Online]. Available: <https://www.mdpi.com/2218-6581/10/4/129>
- [4] O. Onaizah and E. Diller, "Tetherless mobile micro-surgical scissors using magnetic actuation," in *2019 International Conference on Robotics and Automation (ICRA)*, 2019, pp. 894–899.
- [5] Y. Mao, S. Yuan, J. Wang, J. Zhang, and S. Song, "Modeling and control of an untethered magnetic gripper," in *2021 IEEE International Conference on Robotics and Automation (ICRA)*, 2021, pp. 7274–7280.
- [6] T. Enomoto, X. Mao, and U. Satake, "Cutting performance by surgical scissors of tubular soft tissues such as blood vessels," *CIRP Annals*, vol. 70, no. 1, pp. 69–72, 2021.
- [7] F. Pervin and W. W. Chen, "Mechanically similar gel simulants for brain tissues," in *Dynamic Behavior of Materials, Volume 1*, T. Proulx, Ed. New York, NY: Springer New York, 2011, pp. 9–13.
- [8] C. Oates, P. Lucas, and W. Lee, "How brittle are gels?" *Carbohydrate polymers*, vol. 20, no. 3, pp. 189–194, 1993.
- [9] M. Mahvash and V. Hayward, "Haptic rendering of cutting: A fracture mechanics approach," *Haptics-e*, 2001.
- [10] M. Mahvash, L. M. Voo, D. Kim, K. Jeung, J. Wainer, and A. M. Okamura, "Modeling the forces of cutting with scissors," *IEEE Transactions on Biomedical Engineering*, vol. 55, no. 3, pp. 848–856, 2008.
- [11] T. Yang, L. Xiong, J. Zhang, L. Yang, W. Huang, J. Zhou, J. Liu, Y. Su, C. Chui, C. Teo, and S. Chang, "Modeling cutting force of laparoscopic scissors," in *2010 3rd International Conference on Biomedical Engineering and Informatics*, vol. 4, 2010, pp. 1764–1768.
- [12] A. G. Atkins, X. Xu, and G. Jeronimidis, "Cutting, by 'pressing and slicing,' of thin floppy slices of materials illustrated by experiments on cheddar cheese and salami," *Journal of Materials Science*, vol. 39, no. 8, pp. 2761–2766, 2004.
- [13] D. Zhou, M. Claffee, K.-M. Lee, and G. McMurray, "Cutting, 'by pressing and slicing', applied to robotic cutting bio-materials. i. modeling of stress distribution," in *Proceedings 2006 IEEE International Conference on Robotics and Automation, 2006. ICRA 2006.*, 2006, pp. 2896–2901.
- [14] —, "Cutting, 'by pressing and slicing', applied to the robotic cut of bio-materials. ii. force during slicing and pressing cuts," in *Proceedings 2006 IEEE International Conference on Robotics and Automation, 2006. ICRA 2006.*, 2006, pp. 2256–2261.
- [15] S. Kaldor and P. K. Venunod, "Macro-level Optimization of Cutting Tool Geometry," *Journal of Manufacturing Science and Engineering*, vol. 119, no. 1, pp. 1–9, 02 1997. [Online]. Available: <https://doi.org/10.1115/1.2836551>
- [16] B. P. Pereira, P. W. Lucas, and T. Swee-Hin, "Ranking the fracture toughness of thin mammalian soft tissues using the scissors cutting test," *Journal of Biomechanics*, vol. 30, no. 1, pp. 91–94, 1997.
- [17] J. R. Rice, "A Path Independent Integral and the Approximate Analysis of Strain Concentration by Notches and Cracks," *Journal of Applied Mechanics*, vol. 35, no. 2, pp. 379–386, 06 1968. [Online]. Available: <https://doi.org/10.1115/1.3601206>
- [18] H.-J. Kwon, A. D. Rogalsky, C. Kovalchick, and G. Ravichandran, "Application of digital image correlation method to biogel," *Polymer Engineering & Science*, vol. 50, no. 8, pp. 1585–1593, 2010.
- [19] H. Kwon, A. D. Rogalsky, and D.-W. Kim, "On the measurement of fracture toughness of soft biogel," *Polymer Engineering & Science*, vol. 51, no. 6, pp. 1078–1086, 2011.
- [20] J. Blaber, B. Adair, and A. Antoniou, "Ncorr: open-source 2d digital image correlation matlab software," *Experimental Mechanics*, vol. 55, no. 6, pp. 1105–1122, 2015.
- [21] A. Schonewille, "Maximizing workspace accessibility in magnetic actuation of tethered microsurgical tools using non-uniform magnetic fields," M.A.Sc. Thesis, University of Toronto, Toronto, Canada, 2022.
- [22] J. Leclerc, A. Ramakrishnan, N. V. Tsekos, and A. T. Becker, "Magnetic hammer actuation for tissue penetration using a millirobot," *IEEE Robotics and Automation Letters*, vol. 3, no. 1, pp. 403–410, 2018.
- [23] L. M. Barrangou, C. R. Daubert, and E. A. Fogedding, "Textural properties of agarose gels. i. rheological and fracture properties," *Food Hydrocolloids*, vol. 20, no. 2-3, pp. 184–195, 2006.